RESEARCH Revista Mexicana de Física **64** (2018) 216–221 MAY-JUNE 2018

Synthesis, structural characterization and differential thermal analysis of the quaternary compound Ag_2MnSnS_4

G.E. Delgado[a,*], N. Sierralta[b], M. Quintero[c], E. Quintero[c], E. Moreno[c], J.A. Flores-Cruz[d] and C. Rincón[c]
[a]*Laboratorio de Cristalografía, Departamento de Química, Facultad de Ciencias,*
Universidad de Los Andes, Mérida, 5101, Venezuela.
[b]*Grupo de Teoría de la Materia Condensada, Departamento de Física, Facultad de Ciencias,*
Universidad de Los Andes, Mérida 5101, Venezuela.
[c]*Centro de Estudios de Semiconductores, Departamento de Física, Facultad de Ciencias,*
Universidad de Los Andes, Mérida 5101, Venezuela.
[d]*Centro de Investigación en Ciencia Aplicada y Tecnología Avanzada-Instituto Politécnico Nacional,*
Ciudad de México, 11500, México.
**e-mail: gerzon@ula.ve*

Received 18 August 2017; accepted 6 February 2018

The quaternary chalcogenide compound Ag_2MnSnS_4 belonging to the system I_2-II-IV-VI_4 and synthesized by the melt and anneal technique, was characterized by Rietveld refinement of the powder X-ray diffraction data and differential thermal analysis (DTA). It was found that Ag_2MnSnS_4 crystallizes in the orthorhombic space group $Pmn2_1$, with unit cell parameters $a = 8.1705(5)$ Å, $b = 6.9413(5)$ Å, $c = 6.6532(5)$ Å, and $V = 377.33(5)$ Å^3, in a wurtzite-stannite structure. The DTA indicates that this compound melts at 790°C and that the phase relations which occurs in the material would be: $\alpha \rightarrow \alpha + \alpha_1 \rightarrow \alpha_1 \rightarrow \alpha_1 + \beta \rightarrow \beta \rightarrow \beta_1 + L \rightarrow L$, were α is the orthorhombic wurtzite-stannite $Pmn2_1$ structure; α_1 is a high temperature modification; and β and β_1 are the zinc-blende structure and its high-temperature modification, respectively.

Keywords: Chalcogenide; semiconductor; chemical synthesis; X-ray powder diffraction; crystal structure; differential thermal analysis.

PACS: 61.05.cp; 61.50.Nw; 61.66.Fn; 61.40.b

1. Introduction

The family of quaternary I_2-II-IV-VI_4 compounds, where I = Cu or Ag; II = Zn, Cd, Mn, Fe, or Ni; IV = Si, Ge, or Sn; and VI = S, Se, or Te; obtained from the tetrahedrally coordinated derivatives of the II-VI binaries [1], have received considerable attention lately mainly because they can be useful for their potential application as solar-cell absorbers [2-4], photocatalysts for solar water splitting [5] and thermoelectric materials [6-8]. In particular, chalcogenide tin-sulphide complex compounds are very promising for optoelectronics, which is a consequence of high electron-phonon anharmonicity for such kind of materials [9]. One of these materials, Cu2ZnSnS4 has attracted great attention for photovoltaic devices because of its optimum direct band gap energy ($\sim$ 1.5 eV), large absorption coefficient ($\sim 10^{4-6}$ cm^{-1}, naturally abundant and environmentally friendly thin-film solar-cell absorber [10,11]. These quaternaries fulfill the rules of adamantane compound formation, according to which the cation substitution is performed in such a way that the average number of valence electrons per atomic site and the ratio valence electrons to anions, which in diamond-like materials are four and eight, respectively, is preserved [1].

Structural studies carried out on some members of this family indicate that they crystallize in sphalerite or wurtzite derivative structures. In sphalerite derivatives with tetragonal symmetry: in a Cu_2FeSnS_4-type structure (stannite, space group $I\bar{4}2m$) or in a Cu_2ZnSnS_4-type structure (kesterite, space group $I\bar{4}$) [12]. In wurtzite derivatives with orthorhombic symmetry: in a Cu_2CdGeS_4-type structure (wurtzite-stannite, space group $Pmn2_1$) [13] or with monoclinic symmetry (wurtzite-kesterite, space group Pn) [14]. These crystallographic forms are very close to each other with the only difference in the distribution of the cations in the tetrahedral sites (see Fig. 1). Recently, Chen *et al.* [15,16] have shown that there is a clear relationship between the properties of the wurtzite-kesterite and kesterite structures, as well as between wurtzite-stannite and stannite structures.

Several recent studies on the structural characterization and physical properties, including transport properties, of these Cu_2-II-IV-VI_4 [17-28] and Ag_2-II-IV-VI_4 [29-35] quaternary semiconductor chalcogenides have been reported.

On the other hand, I_2-II-IV-VI_2 semiconducting compounds in which the II cation is a paramagnetic ion, as Mn^{+2}, Fe^{+2}, Co^{+2} or Ni^{+2}, known as semimagnetic materials, have also received considerable attention because magneto-optical effects larger than those observed in $II_{1-x}Mn_x$-V_{I2} alloys could be obtained in such quaternaries [36]. One of them, Ag_2MnSnS_4 could be of interest because it exhibits antiferromagnetic behavior [37]. Concerning to its crystal structure, discrepancy exists in the scarce information reported the literature. According to Lamarche *et al.* [37], this compound crystallizes with orthorhombic symmetry and unit cell parameters $a = 8.019$ Å, $b = 6.964$ Å, $c = 6.527$ Å, without defining its space group or structure. However, it has been more recently reported, with no structural details [38], that

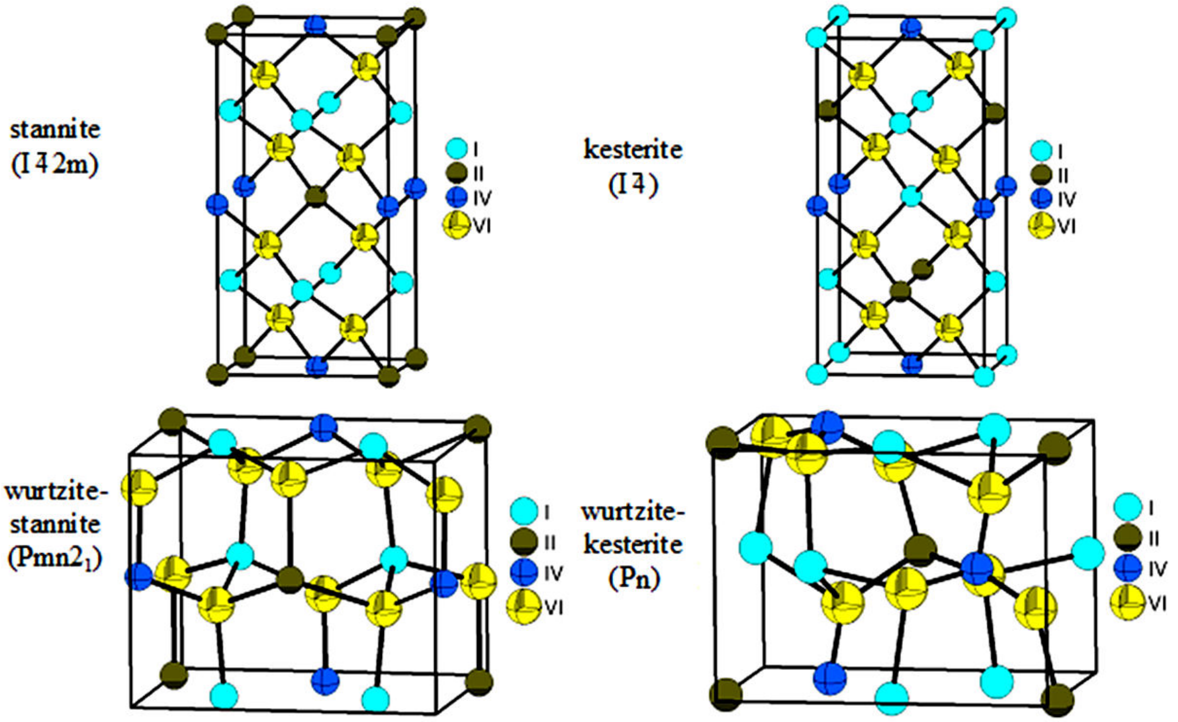

FIGURE 1. Unit cell diagram of the stannite, kesterite, wurtzite-stannite and wurtzite-kesterite structures showing the cation and anion distribution in the I_2-II-IV-VI_4 family of compounds.

Ag_2MnSnS_4 crystallizes in the monoclinic space group Pn, with unit cell parameters $a = 6.696(1)$ Å, $b = 6.991(1)$ Å, $c = 8.222(2)$ Å, $\beta = 90.00(3)^\circ$ (pseudo-orthorhombic).

Furthermore, Ag_2MnSnS_4 is one of the three sulfide minerals containing silver and tin found in nature. They are the hocartite, Ag_2FeSnS_4, found in Bolivia in 1967 [39], the pirquitasite, Ag_2ZnSnS_4, found in Argentina in 1980 [40], and the agmantinite, Ag_2MnSnS_4, found in Perú in 2014 [41], whose name has been recently approved by the Commission on New Minerals, Nomenclature and Classification of the International Mineralogical Association [41].

In view of the considerable importance of such semimagnetic compound, in this work we report the synthesis, thermal analysis and crystal structure characterization of the I_2-II-IV-VI_4 Ag_2MnSnS_4 semimagnetic compound.

2. Experimental

2.1. Synthesis

The sample was synthesized by the melt and anneals technique. Highly pure components (silver 99.98%, manganese 99.97%, tin 99.99%, and sulphur 99.99) of 1 g sample were sealed under vacuum ($\approx 10^{-5}$ Torr) in a small quartz ampoule, and then the components were heated up to 200°C and kept for about 1-2 h. The temperature was then raised to 500°C using a rate of 40°C/h, and held at this temperature for 14 hour. After, the sample was heated from 500°C to 800°C at a rate of 30°C/h and kept at this temperature for another 14 hours. Then it was raised to 1150°C at 60°C/h, and the components were melted together at this temperature. The furnace temperature was brought slowly (4°C/h) down to 600°C, and the sample was annealed at this temperature for 1 month. Finally, the sample was slowly cooled to room temperature using a rate of about 2°C/h.

2.2. Chemical Analysis

The stoichiometric relation of the sample was investigated by SEM technique, using a Hitachi S2500 microscope equipped with a Kedex EDX accessory. Three different regions of the ingot were scanned and the average atomic percentages are as follows: Ag (25.2%), Mn (11.1%), Sn (11.3%) and S (52.4%). The error in standardless analysis was around 5%. These values are in good agreement with the ideal composition 2:1:1:4.

2.3. Differential thermal analysis (DTA)

Phase transition temperatures were obtained in the temperature range between 20 to 1150°C, using a Perkin-Elmer DTA-7 with aluminum and gold used as reference materials. The charge was of powdered alloy of approximately 100 mg weight. Both heating and cooling runs were carried out on each sample. The average rates of these runs being approximately 10°C/min. The error in determining these temperatures is of about ±10°C.

2.4. X-ray powder diffraction (XRPD)

For the X-ray analysis, a small quantity of the sample, cut from the ingot, was ground mechanically in an agate mortar and pestle, and sieved to a grain size of less than 10 μm. The XRPD data was collected at 293(1) K, in θ/θ reflection mode using a Siemens D5005 diffractometer equipped with an X-ray tube (CuKα radiation: $\lambda = 1.5418$ Å; 40 kV, 30 mA). The specimen was scanned from 10°-80° 2θ, with a step size of 0.02° and counting time of 10 s. Quartz was used as an external standard.

3. Results and Discussion

3.1. Differential thermal analysis

DTA runs were carried out on the sample as indicated above. The transition temperatures as well as the type of melting were obtained from the peaks on the DTA heating and cooling curves. Each transition temperature was determined from the base intercept of the tangent to the leading edge of the peak in the differential signal. The value of the melting point temperature, denoted as TM, obtained from the peaks on the DTA curve, is given in Fig. 2, which shows the thermogram for Ag_2MnSnS_4.

Three transitions are observed in both heating and cooling runs. These appear at about 477, 640 and 790°C, and at about 973, 700 and 592°C, in these curves, respectively. It can also be seen, that the compound melts congruently at about 973°C. Hence, the effect observed at 973°C corresponds to the transition from (L + β_1) to the liquid state L. Here, β_1 is a zinc-blende (ZB) structure high-temperature modification. The effect observed at 790°C corresponds to the liquid-line, *i.e.*, to the peritectic decomposition of the Ag_2MnSnS_4 from β (other ZB phase high temperature modification) to L + β_1. On the other hand, the peaks at 640 and 700°C, in the heating curve, are related to the peritectic decomposition of the compound from α_1, which is a wurtz-stannite phase high temperature modification, to $\beta + \alpha_1$, and to the solid-solid transformation from $\beta + \alpha_1$ to β, respectively. In addition, the peaks at 592 and 640°C correspond to the peritectic decomposition of the Ag_2MnSnS_4, from $\alpha_1 + \alpha$ to solid α_1, and to the transition from α_1 to $\beta + \alpha_1$, respectively. The transition at about 477°C, observed in heating curve, corresponds to the peritectic decomposition of the room temperature α-Ag_2MnSnS_4 phase with wurtz-stannite ($Pmn2_1$) structure, to $\alpha + \alpha_1$. Finally, the sequence of phase relations for this compound from low to high temperatures should be: $\alpha \rightarrow \alpha + \alpha_1 \rightarrow \alpha_1 \rightarrow \alpha_1 + \beta \rightarrow \beta \rightarrow \beta_1 + \mathrm{L} \rightarrow \mathrm{L}$.

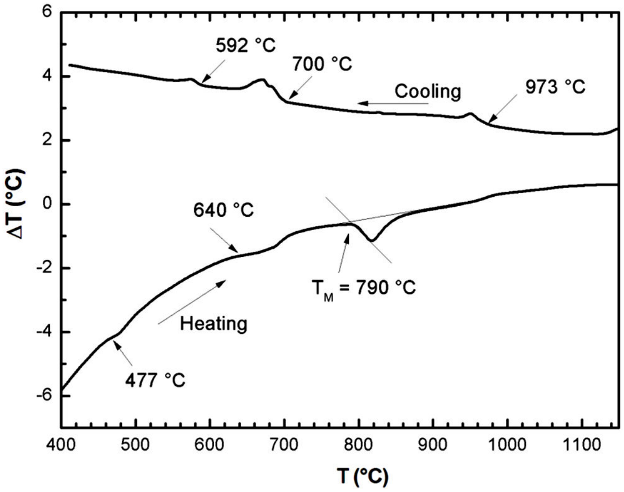

FIGURE 2. DTA thermogram for Ag_2MnSnS_4. The direction of heating run, or cooling run, is indicated by the corresponding arrow.

3.2. X-ray powder diffraction analysis

Figure 3 shows the resulting X-ray powder diffractogram for the Ag_2MnSnS_4 compound. The X-ray powder pattern show a single phase. The 20 first peak positions were indexed using the program Dicvol04 [42], which gave a unique solution in an orthorhombic cell with parameters $a = 8.170(1)$ Å, $b = 6.940(1)$ Å, and $c = 6.650(1)$ Å. The lack of systematic absence condition $h + k + l$, in the general reflections of the type hkl, indicated a P-type cell. By analyzing the crystallographic characteristics of Ag_2MnSnS_4 with those of other I_2-II-IV-VI_4 related compounds, taking in account the sample composition, cell parameters and lattice-type, it is found that this material is isomorphic with Ag_2CdGeS_4 [29] which crystalize with wurtzite-stannite structure (space group $Pmn2_1$) [13]. So, in order to refine the structural parameters of Ag_2MnSnS_4, the space group $Pmn2_1$ (N° 31) and the atomic position parameters of Ag_2CdGeS_4 were taken as the starting values.

The Rietveld refinement [43] was performed using the Fullprof program [44]. The indexed unit cell results were taken as starting parameters. The angular dependence of the peak full width at half maximum (FWHM) was described by

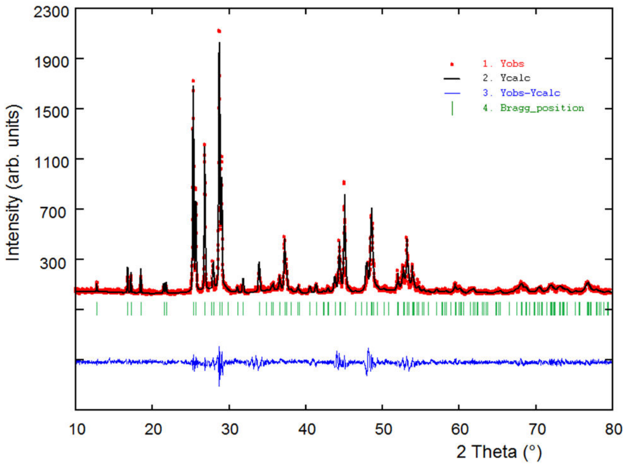

FIGURE 3. Final Rietveld plot showing the observed, calculated and difference pattern for the Ag_2MnSnS_4 compound. The Bragg reflections for both phases are indicated by vertical bars.

TABLE I. Results of Rietveld refinement for Ag_2MnSnS_4.

Molecular formula	Ag_2MnSnS_4	D_{calc}	4.55 (g/cm^3)
Molecular weight	517.7 (g/mol)	N° step intensities	4001
Crystal system	Orthorhombic	N° independent reflections	145
Space group	$Pmn2_1$ (N° 31)	Peak-shape profile	Pseudo-Voigt
Z	2		
a	8.1705(5) Å	R_{exp} 9.6 %	
b	6.9413(5) Å	R_p	10.3 %
c	6.6532(5) Å	R_{wp} 11.8 %	
V	377.33(5)	S	1.2

R_{exp} = 100 [(N-P+C)/$\sum_W (y^2_{obs})]^{1/2}$ N-P+C is the number of degrees of freedom, R_p = 100 $\sum \mid y_{obs} - y_{calc} \mid / \sum \mid y_{obs} \mid$
R_{wp} = 100 $\sum_w \mid y_{obs} - y_{calc} \mid / \sum \mid y_{obs} \mid]^{1/2}$ S= [R_{wp}/R_{exp}]

TABLE II. Atomic coordinates, occupancy factors and isotropic temperature factor for Ag_2MnSnS_4.

Atom	Ox.	Wyck.	x	y	z	foc	B (Å^2)
Ag	+1	$4b$	0.256(2)	0.317(2)	0	1	0.6(1)
Mn	+2	$2a$	0	0.848(2)	0.988(2)	1	0.6(1)
Sn	+4	$2a$	0	0.185(2)	0.491(2)	1	0.6(1)
S1	-2	$4b$	0.237(2)	0.325(2)	0.387(2)	1	0.6(1)
S2	-2	$2a$	0	0.186(2)	0.821(2)	1	0.6(1)
S3	-2	$2a$	0	0.884(2)	0.365(2)	1	0.6(1)

TABLE III. Distance lengths (Å) and bond angles (°) for Ag_2MnSnS_4.

Ag-S1	2.58(1)	Mn-S1^{iii}	2.55(2)	Sn-S1	2.27(2)
Ag-S1^{i}	2.60(2)	Mn-S1^{vi}	2.55(2)	Sn-S1^{vii}	2.27(2)
Ag-S2^{ii}	2.57(2)	Mn-S2^{iv}	2.60(2)	Sn-S2	2.20(2)
Ag-S3^{i}i	2.59(2)	Mn-S3^{v}	2.52(2)	Sn-S3^{viii}	2.25(2)
S1-Ag-S1^{i}	105.6(4)	S1-Ag-S2^{ii}	114.9(3)	S1-Ag-S3^{i}	113.8(3)
S2^{ii}-Ag-S1^{i}	102.8(3)	S1^{i}-Ag-S3^{i}	113.4(3)	S2^{ii}-Ag-S3^{i}	105.9(3)
S1^{iii}-Mn-S1^{vi}	114.7(5)	S1^{iii}-Mn-S2^{iv}	108.2(3)	S2^{iv}-Mn-S1^{vi}	108.2(3)
S3^{v}-Mn-S1^{iii}	108.0(3)	S3^{v}-Mn-S1^{vi}	108.0(3)	S3^{v}-Mn-S2^{iv}	109.7(7)
S2-Sn-S1	107.6(3)	S2-Sn-S3^{viii}	112.0(8)	S1-Sn-S3^{viii}	106.5(4)
S1^{vii}-Sn-S2	107.6(3)	S1^{vii}-Sn-S1	116.7(6)	S1^{vii}-Sn-S3^{viii}	106.5(4)

Symmetry codes: (i) $0.5 - x, 1 - y, -0.5 + z$; (ii) $x, y, -1 + z$; (iii) $-0.5 + x, 1 - y, 0.5 + z$; (iv) $x, 1 + y, z$; (v) $x, y, 1 + z$; (vi) $0.5 - x, 1 - y, 0.5 + z$; (vii) $-x, y, z$; (viii) $x, -1 + y, z$.

the Cagliotti's formula [45]. The parameterized Thompson-Cox-Hastings pseudo-Voigt profile function [46] was used for the simulation of the peak shapes. The background of the XRD data was refined with a polynomial with six coefficients. The thermal motion of the atoms was described by one overall isotropic temperature factor. A total of 23 parameters of the Ag_2MnSnS_4 compound, including peak shape, scale factor, cell, atomic coordinates, isotropic displacement and full-width at half-maximum (FWHM) parameters, were refined. The final Rietveld refinement led to agreement factors of: R_p = 10.3%, R_{wp} = 11.8%, R_{exp} = 9.6%, and S = 1.2, for 4001 step intensities and 145 independent reflections.

The results of the Rietveld refinement are summarized in Table I. Figure 3 shows the observed calculated and difference profile for the final cycle of the refinement. Atomic coordinates, occupancy factors and isotropic temperature factor are given in Table II. Bond distances and angles are given in Table III. Figure 4 shows the unit cell diagram for Ag_2MnSnS_4.

Ag_2MnSnS_4 crystallize with orthorhombic symmetry, space group $Pmn2_1$, and unit cell parameters: a=$8.1705(5)$ Å, b=$6.9413(5)$ Å, c=$6.6532(5)$ Å, and V=$377.33(5)$ Å^3 in a wurtzite-stannite structure. This structure can be described as a hexagonal, closest-packed array of sulfur anions with

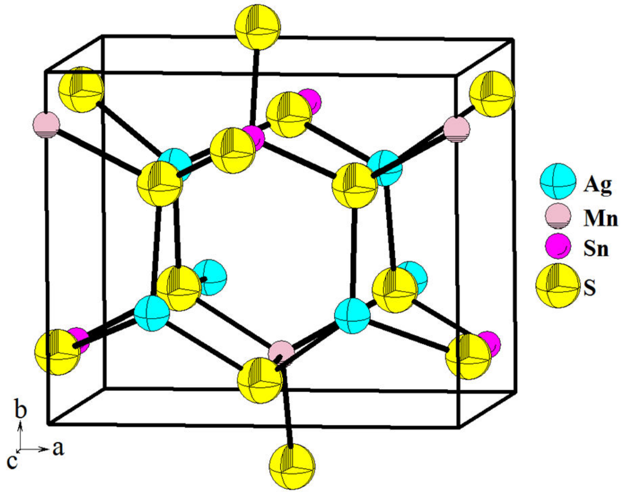

FIGURE 4. Unit cell diagram of Ag_2MnSnS_4 viewed in the *ba* plane of the space group $Pmn2_1$.

Ag^+, Mn^{+2} and Sn^{4+} occupying tetrahedral holes, and is characterized by a three-dimensional arrangement of slightly distorted AgS_4, MnS_4 and SnS_4 tetrahedra connected by corners. All S atoms are surrounded by two Ag atoms and by one Mn and one Sn atom, and each cation is coordinated by 4 anions. This array is expected for adamantane compounds [1].

The tetrahedrons containing the Sn atoms [mean S…S distance 3.67(2) Å] are slightly smaller than those containing the Mn atoms [means S…S distance 4.16(2) Å] and Ag atoms [mean S…S distance 4.22(2) Å] respectively. The interatomic distances are shorter than the sum of the respective ionic radii ($r\text{Ag}^+$ = 1.14, $r\text{Mn}^{2+}$ = 0.80, $r\text{Sn}^{4+}$ = 0.69, $r\text{S}^{2-}$ = 1.70 Å) for structures tetrahedrally bonded [47].

The mean bond distance values for Ag-S, Mn-S and Sn-S, given in Table III, agree well with the distances observed in other adamantane compounds as Ag_2CdSnS_4 [9], Ag_2CdGeS_4 [29], Ag_2CdSnS_4 [30], Ag_2ZnSiS_4 [32], $AgCd_2GaS_4$ [48], Ag_2ZnGeS_4 [49], $MnIn_2S_4$ [50], $AgInS_2$ and $AgIn_5S_8$ [51].

In addition, the Debye temperature θ_D, which is an important parameter in the understanding of thermal and electrical properties of semiconducting materials, can be estimated for this compound by using the Lindemann's expression $\theta_D \approx C(T_M/\bar{W})^{1/2}(1/a_e)$ [52]. Here, $\bar{W} = W/n$, W is the molecular weight, n is the number of atoms per molecule ($n = 8$ for Ag_2MnSnS_4), C is a constant ($C \approx 300$ for I_2-II-IV-VI_4 tetrahedral bonded quaternary compounds [24]), and ae is the effective lattice parameter $a_e = (V/Z)^{1/3}$, where V is the volume of unit cell (in Å^3) and Z the number of molecules per cell ($Z = 2$). For Ag_2MnSnS_4, from the calculated value $a_e = 5.7354$ Å, we obtain $\theta_D 212$ K. This value is in good agreement with those reported for the related Cu_2Mn-IV-VI_2 semimagnetic semiconductor compounds, which vary from 185 to 310 K [24].

4. Conclusions

The quaternary chalcogenide compound Ag_2MnSnS_4 crystallizes in the wurtzite-stannite structure, space group $Pmn2_1$, characterized by a three-dimensional arrangement of slightly distorted AgS_4, MnS_4 and SnS_4 tetrahedras connected by corners. The DTA indicates that this compound melts at 790°C.

Acknowledgments

This work was supported by CDCHT-ULA FONACIT (Grant LAB-97000821).

1. E. Parthé: Wurtzite and Sphalerite Structures. In: J.H. Westbrook, R.L. Fleischer (Eds), *Intermetallic Compounds, Principles and Applications*. **Vol. 1**, John Wiley & Sons, Chichester, UK, Chap. 14 (1995).
2. Q. Guo, W.W. Hillhouse, R. Agrawal, *J. Am. Chem. Soc.* **131** (2009) 11672.
3. S. Ahn *et al.*, *App. Phys. Letters*, **97** (2010) 021905.
4. T.K. Todorov, K.B. Reuter, and D.B. Mitzi, *Adv. Mater*. **22** (2010) E156.
5. I. Tsuji, Y. Shimodaira, H. Kato, H. Kobayashi, and A. Kudo, *Chem. Mater*. **22** (2010) 1402.
6. X.Y. Shi, F.Q. Huang, M.L. Liu, and L.D. Chen, *App. Phys. Letters*, **94** (2009) 122103.
7. C. Sevik and T. Cagin, *Phys. Rev. B*, **82** (2010) 045202.
8. M. Ibáñez *et al.*, *Chem. Mater*. **24** (2012) 562.
9. G.E. Davydyuk *et al.*, *Opt. Mater*. **33** (2011) 1302.
10. W. Liu *et al.*, *Thin Solid Films* **535** (2013) 39.
11. M. Wei *et al.*, *Mater. Letters* **79** (2012) 177.
12. S.R. Hall, J.T. Szymanski, and J.M. Stewart, *Can. Mineral*. **16** (1978) 131.
13. E. Parthé, K. Yvon, and R.H. Deitch, *Acta Cryst. B* **25** (1969) 1164.
14. C.A. Joubert-Bettan, R. Lachenal, E.F. Bertaut, and E. Parthé, *J. Solid State Chem*. **1** (1969) 1.
15. S. Chen, X.G. Gong, A. Walsh, and S-H. Wei, *Phys. Rev. B*, **79** (2009) 165211.
16. S. Chen *et al.*, *Phys. Rev. B*, **82** (2010) 195203.
17. E. Quintero *et al.*, *Phys. B: Cond. Matter*, **320** (2002) 384.
18. G.E. Delgado, E. Quintero, R. Tovar, and M. Quintero, *Cryst. Res. Technol*. **39** (2004) 807.
19. E. Quintero *et al.*, *J. Alloys Comp*. **432** (2007) 142.
20. M. Quintero *et al.*, *Ciencia*, **15** (2007) 222.
21. D. Caldera *et al.*, *J. Alloys Comp*. **457** (2008) 221.

22. E. Moreno *et al*., *J. Alloys Comp*. **486** (2009) 212.
23. C. Rincón *et al*., *Solid State Comm*. **151** (2011) 947.
24. M. Quintero *et al*., *Rev. LatinAm Met. Mater*. **34** (2014) 28.
25. F. López-Vergara, A. Galdámez, V. Manríquez, P. Barahona, and O. Peña, *phys. stat. sol. (b*) **251** (2014) 958.
26. Y. Dong, L. Wojtas, J. Martin, and G.S. Nolas, *J. Mater. Chem*. **3** (2015) 10436.
27. K. Wei and G.S. Nolas, *J. Solid State Chem*. **226** (2015) 215.
28. O.V. Parasyuk, L.D. Gulay, L.V. Piskach, and I.D. Olekseyuk, *J. Alloys Comp*. **397** (2005) 95.
29. O.V. Parasyuk, L.V. Piskach, I.D. Olekseyuk, and V.I. Pekhnyo, *J. Alloys Comp*. **335** (2002) 176.
30. G.E. Davydyuk *et al*., *Opt. Mater*. **33** (2011) 1302.
31. C.D. Brunetta, W.C. Minsterman, C.H. Lake, and J.A. Aitken, *J. Solid State Chem*. **187** (2012) 177.
32. C.D. Brunetta, K. Balamurugan, K.A. Rosmus, and J.A. Aitken, *J. Alloys Comp*. **516** (2012) 65.
33. C.D. Brunetta *et al*., *J. Alloys Comp.* **574** (2013) 495.
34. K. Wei and G.S. Nolas, *ACS App. Mater. & Interfaces* **7** (2015) 9752.
35. K. Wei, A.R. Khabibullin, T. Stedman, L.M. Woods, and G.S. Nolas, *J. Appl. Phys*. **122** (2017) 105109.
36. Y. Shapira *et al*., *Phys. Rev. B* **37** (1988) 411.
37. M. Lamarche, A. Willsher, L. Chen, G. Lamarche, and J.C. Woolley, *J. Solid State Chem*. **94** (1991) 313.
38. S. Greil and A. Pfitzner, *Z. Anorg. Allg. Chem*. **638** (2012) 1570. Abstracts of the 16th Conference of the GDCh Division for Solid State Chemistry and Materials Research, Darmstadt, Germany, Sept. 2012.
39. R. Caye, Y. Laurent, P. Picot, R. Pierrot, and C. Levy, *Bull. Soc. Fran. Minér. Crist*. **91** (1968) 383.
40. Z. Johan, and P. Picot, *Bull. Minér*. **105** (1982) 229.
41. F.N. Keutsch, D. Topa, R. Takagi, E. Makovicky, and W. Paar, Agmantinite IMA 2014-083 Commission on New Minerals, *Nomenclature and Classification (CNMNC) Newsletter* No. 23, Feb. 2015, page 57. *Mineral. Mag.* **79** (2015) 51.
42. A. Boultif and D. Louër, *J. App. Cryst*. **37** (2004) 724.
43. H.M. Rietveld, *J. App. Cryst*. **2** (1969) 65.
44. J. Rodriguez-Carvajal, *Phys. B: Cond. Matter* **192** (1993) 55.
45. G. Cagliotti, A. Paoletti, and F.P. Ricci, *Nucl. Instrum*. **3** (1958) 223.
46. P. Thompson, D.E. Cox, and J.B. Hastings, *J. App. Cryst*. **20** (1987) 79.
47. S.D. Shannon, *Acta Cryst. A* **32** (1976) 751.
48. N.V. Pervukhina, V.V. Atuchinb, and O.V. Parasyuk, *Acta Cryst. E* **61** (2005) i91.
49. O.V. Parasyuk, A.O. Fedorchuk, Yu.M. Kogut, L.V. Piskach, and I.D. Olekseyuk, *J. Alloys Comp.* **500** (2010) 26.
50. V. Sagredo, M.C. Morón, L. Betancourt, and G.E. Delgado, *J. Mag. Mag. Mater*. **312** (2007) 294.
51. G.E. Delgado, A.J. Mora, C. Pineda, and T. Tinoco, *Mater. Res. Bull*. **36** (2001) 2507.
52. P. Deus, H.A. Schneider, and U. Voland, *Cryst. Res. Technol*. **16** (1981) 941.